Liquid Crystals, Vol. 32, No. 2, February 2005, 267–275

Cell gap-dependent transmission characteristics of a fringe-electric field-driven homogeneously aligned liquid crystal cell, for a liquid crystal with negative dielectric anisotropy

SONG HEE JUNG†, HYANG YUL KIM†‡, MYOUNG-HOON LEE†, JOHN MOON RHEE† and SEUNG HEE LEE*†

†School of Advanced Materials Engineering, Research Center of Advanced Materials Development, Chonbuk National University, Chonju-si, Chonbuk 561-756, Korea

‡Panel Design Group, BOE-HYDIS Technology Co. Ltd., Ichon-si, Kyunggi-do 467-701, Korea

(*Received 27 February 2004; in final form 26 July 2004; accepted 14 August 2004*)

Transmittance characteristics were studied as a function of cell gap for a homogeneously aligned liquid crystal (LC) cell driven by a fringe-electric field—named fringe-field switching (FFS) mode. The light efficiency of a conventional LC cell using in-plane switching and twisted nematic modes, where the LC director is determined by competition between elastic energy and electrical energy, does not depend on cell gap as long as the cell retardation value remains the same; i.e. only dielectric torque contributes to the deformation of the LC director. However, the transmittance of the FFS mode is dependent on the cell gap such that it decreases as the cell gap decreases, although the cell retardation value remains the same. This unusual behaviour (unlike that of conventional LC cells) arises because in the device the elastic and dielectric torques have the role of determining the LC director, such that the driving voltage giving rise to maximum transmittance becomes strongly dependent on the electrode position when the cell gap is as small as 2 μm. In addition, the LCs at the centre of the pixel and common electrodes are not sufficiently twisted because of a competition between the two elastic forces, which tries to twist the LCs in plane and hold them in their initial state by surface anchoring.

1. Introduction

The image quality of liquid crystal displays (LCDs) has improved greatly with the development of new LC modes such as the in-plane switching (IPS) mode [1–4] and fringe-field switching (FFS) mode [5, 6]. In these modes the LC director rotates almost in plane. The IPS mode was the first to exhibit high image quality among LCDs although they possessed intrinsically low transmittance. The FFS mode was the first to simultaneously utilize a high transmittance and a wide viewing angle.

In the initial state for both devices, the LCs are homogeneously aligned, and the in-plane or fringe electric field drives the LCs to rotate. However, the different shapes of the driving fields produce different electro-optic characteristics in each device [7]. Furthermore, in the FFS mode, the electro-optical characteristics (i.e. light efficiency), driving voltage [8] and the stability of the voltage-dependent LC dynamics [9], are strongly dependent on the dielectric anisotropy of the LC. This difference also causes behaviour changes when the display experiences external pressure [10].

In LCDs, the light efficiency of the LC cell depends on the cell retardation value, which is a multiplication of the cell gap d and the birefringence Δn of the LC. Therefore, the light efficiency of conventional LC cells such as twisted nematic (TN) [11] and IPS is dependent not only on the cell gap but also on the birefringence. Therefore, it remains the same as long as the cell retardation value remains constant, even though the cell gap changes. However, we found that light efficiency in the FFS mode was dependent on the cell gap, which may be caused by the different switching mechanism of the FFS mode compared with other devices. In this study, we investigated the light efficiency of the FFS mode in relation to cell gap when using a LC with negative dielectric anisotropy (-LC) and found the origin of the behaviour using simulations and experiments.

*Corresponding author. Email: lshl@chonbuk.ac.kr

Liquid Crystals
ISSN 0267-8292 print/ISSN 1366-5855 online © 2005 Taylor & Francis Group Ltd
http://www.tandf.co.uk/journals
DOI: 10.1080/02678290412331329233

2. Switching principle of the fringe-field switching (FFS) mode

The normalized light transmission of a device with a birefringent LC medium under a crossed polarizer is given by:

$$T/T_o = sin^2(2\psi(V))sin^2(\pi d\Delta n/\lambda) \quad (1)$$

where ψ is a voltage-dependent angle between the transmission axes of the crossed polarizers and the LC director, and λ is the wavelength of the incident light.

In the FFS mode, the LCs are homogeneously aligned in the initial state under crossed polarizer with an optic axis of the LC coincident with one of the polarizer axes so that ψ is zero and the cell appears black, as shown in figure 1. With respect to electrode structure, the FFS device has electrodes only on the bottom substrate. A common electrode exists as a plane and a pixel electrode exists as a slit form with a separation between pixel electrodes. A passivation layer is positioned between the common and the pixel electrodes; at this position both electrodes should be transparent. With this electrode structure, a fringe electric field having both horizontal (E_x) and vertical (E_z) field components is generated when the voltage is applied as shown in figure 1. To understand the electro-optic characteristics of the new device, first, we calculated the field distribution along the horizontal axis at three vertical distances, 0.4, 2 and 3.6 μm, from the bottom surface. Figure 2 shows the distribution of the field intensity of the vertical and horizontal components along the horizontal direction in the FFS devices when a voltage of 4.5 V with respect to one common electrode was applied to all pixel electrodes. As shown, the field intensity of E_x around the edge of the pixel electrodes is maximum and rapidly drops to zero above the centre of the electrodes. The field intensity also decreases rapidly on moving away from the electrode surface. This implies that deformation of the LC is much greater near the bottom surface than near the top surface. In the case of E_z, maximum field intensity exists near the region between the edge and the centre of the electrodes, although it is much weaker than that of E_x. Similarly, it also decreases on moving away from the electrode surface. Such a field distribution, which is dependent on electrode position, causes the LCs to deform differently depending on electrode position. Regardless of the deformation, the fringe-

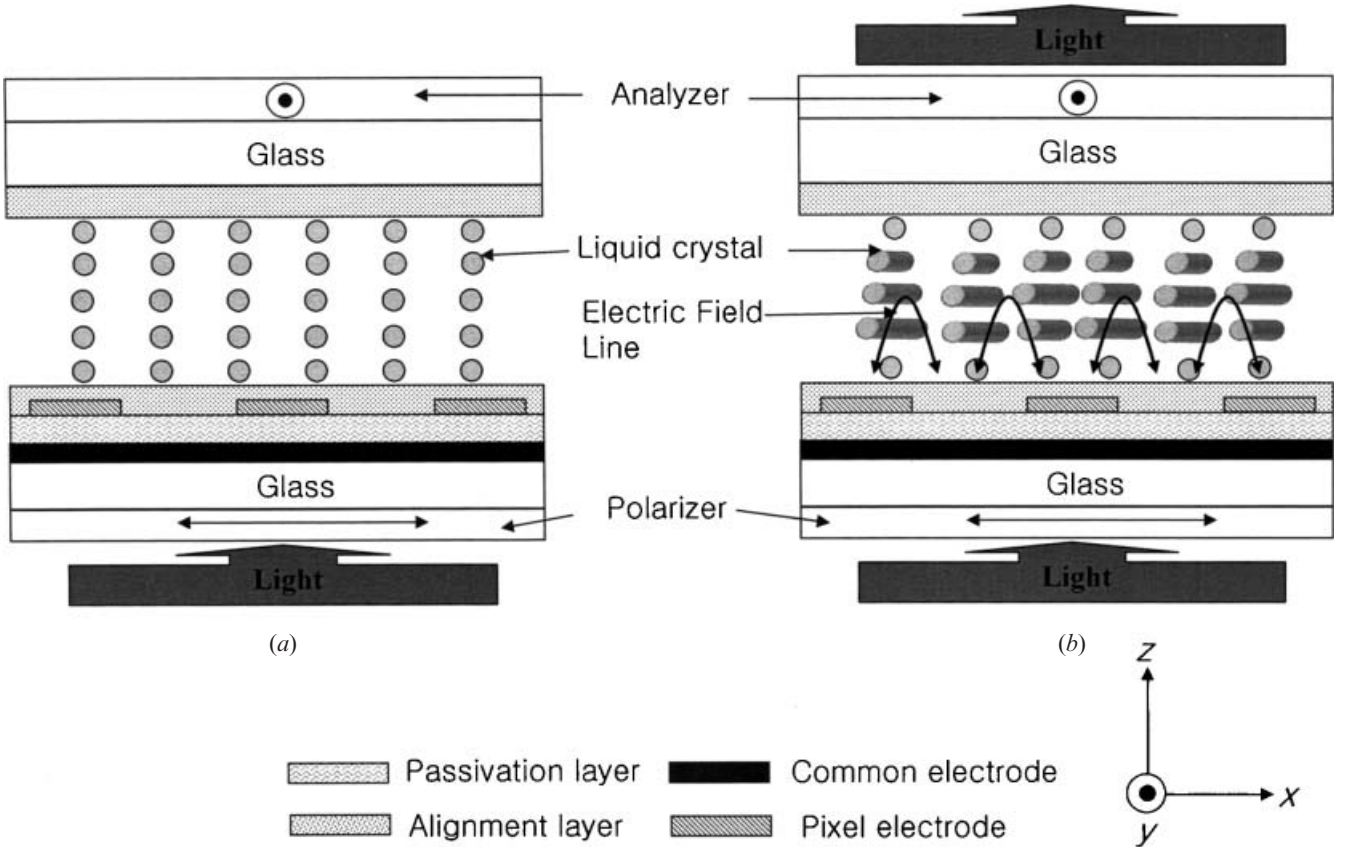

Figure 1. Schematic of cell structure and configuration of the LC molecules in the white state of the FFS mode using the -LC.

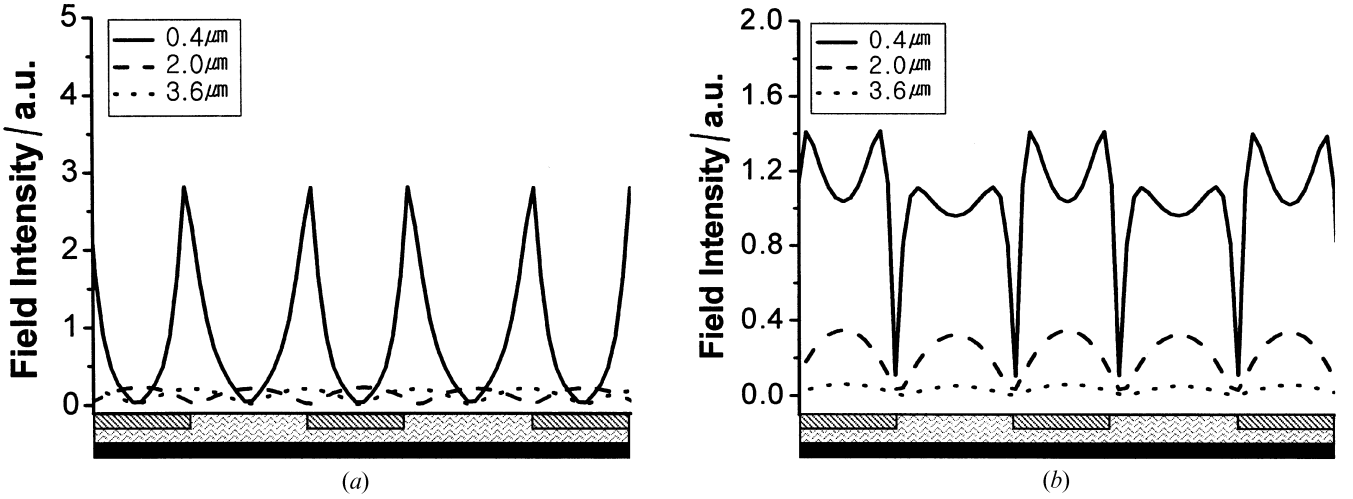

Figure 2. Field distribution of (*a*) the horizontal and (*b*) the vertical component in the FFS device along the horizontal plane at several vertical distances.

electric field still causes the LC to rotate almost in plane above the whole electrode surface, resulting in high transmittance; furthermore, the degree of transmittance along the electrode position is dependent on electrode width and the distance separating them [12].

Figure 3 shows how transmittance along electrode position occurs as a function of relaxation time when an operating voltage is applied. For the calculation, we used commercially available software 'LCD Master' (Shintech, Japan), where the motion of the LC director is calculated based on the Eriksen–Leslie theory, and 2×2 Jones Matrix is applied for optical transmittance calculation [13]. Here, the electrode and passivation thicknesses are 400 and 4 500 Å, respectively. The pixel electrode width and the distance between them are 3 and 4.5 μm, respectively. An LC having negative

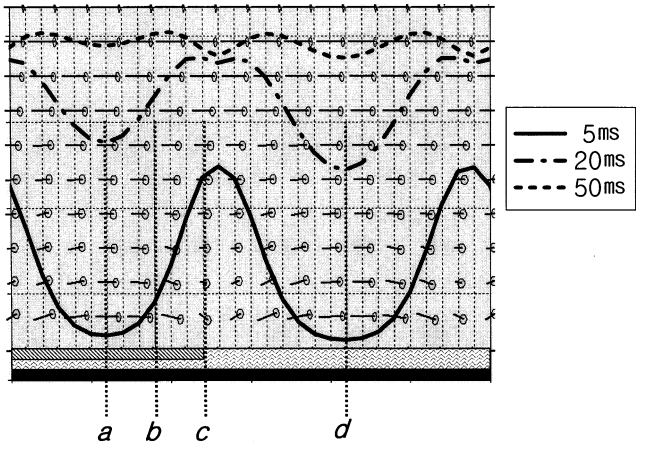

Figure 3. Distribution of the LC molecules and corresponding transmittance as a function of rise times in the white state of the FFS mode using the -LC.

dielectric anisotropy ($\Delta n = 0.077$ at $\lambda = 589$ nm, $\Delta\varepsilon = -4$, $K_1 = 13.5$ pN, $K_2 = 6.5$ pN, $K_3 = 15.1$ pN) and a cell gap of 4 μm is used. The initial rubbing direction is 78° with respect to the *x*-direction. As can be seen from figure 3, when an operating voltage is applied, after 5 ms the transmittance increases strongly near the electrode edge (position *c*) but is almost zero at the centre of the pixel and counter electrode (positions *a* and *d*); after a further relaxation time of 20 ms, transmittance takes place above the whole electrode surface including positions *a* and *b* but still oscillates along the electrode. After 50 ms, transmittance takes place over the whole area, creating high transmittance, even though the accompanying degree of deformation of the LC differs depending on electrode position, because of different torques acting on the LCs. From the time-dependent transmittance profile, it can be seen that at the electrode edge the LC is rotated first by a strong dielectric torque $\Gamma_{\text{dielectric}}$ between E_x and the LC director **n**, and then the LC at the centre of the electrode is rotated by the twisting elastic force given by neighbouring molecules, as shown in figure 4. If the LC director $\mathbf{n}_1$ (located at position *b*) surrounding the LC director $\mathbf{n}_2$ (located at position *a*) is rotated by $\Gamma_{\text{dielectric}}$, the LC director $\mathbf{n}_2$ will try to rotate along the LC director $\mathbf{n}_1$ because of elastic torque Γ_{elastic}, which explains the deformation of the LCs at positions *a* and *d*. Consequently, in FFS mode the dielectric torque $\Gamma_{\text{dielectric}}$ and the elastic torque Γ_{elastic} have a switching role depending on horizontal position, while in the conventional TN and IPS device, all the LC orientations are determined by a competition between elastic and electrical energies, i.e. the dielectric torque contributes to deform the LC. Therefore, in the FFS device the total bulk torque Γ_{total} per unit volume

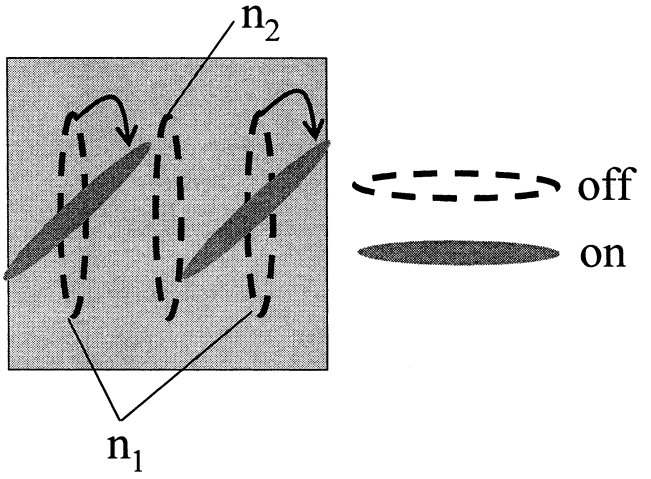

Figure 4. Schematic view of the LCs above a pixel electrode in top view, describing the elastic torque acting on the LC at the centre.

needed to distort the LCs in a homogeneously aligned state can be described as:

$$\Gamma_{\text{total}} = \Gamma_{\text{dielectric}} + \Gamma_{\text{elastic}} = \Delta\varepsilon(\mathbf{n}\cdot\mathbf{E})\mathbf{n}\times\mathbf{E} + F(\mathbf{n_1}\cdot\mathbf{n_2})\mathbf{n_1}\times\mathbf{n_2} \quad (2)$$

where **n** is the LC director homogeneously aligned in its initial state and F is the intermolecular force per unit area. From equation (2), one can deduce that Γ_{elastic} is zero when the angle between two LC directors is 0° or 90°, but the LC at position a will be twisted as long as the two directors make an arbitrary angle not equal to 0° or 90°.

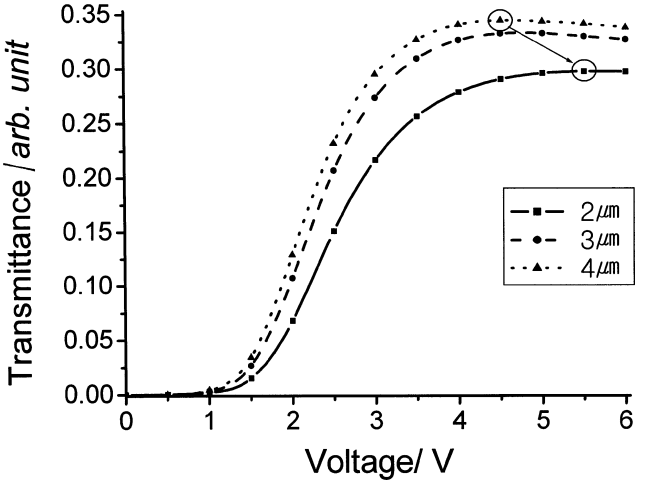

Figure 5. Calculated voltage-dependent transmittance curves for cells with different cell gaps.

3. Calculated results and discussion

As mentioned already, in the FFS device, the transmittance is dependent on electrode position. We also investigated the change of transmittance along the electrode position as a function of cell gap while keeping cell retardation values for all cells the same. Figure 5 shows voltage-dependent transmittance (V–T) curves when the cell gap varies from 4 to 2 μm. Here, electrode structure and the physical properties of the LC are the same as the data described previously, while the birefringence of the LC is varied to keep the cell retardation value the same as described already. The rubbing direction, an optic axis of the LC, is 12° from the E_x, and the surface tilt angle is 2°. As indicated, the V–T curve shifts to right; that is, the threshold voltage (V_{th}) and the operating voltage (V_{op}) at which the maximum transmittance occurs, increase as the cell gap decreases. Interestingly, transmittance is reduced as the cell gap decreases from 4 to 2 μm. The increase of V_{th} with decreasing cell gap is similar to that shown in IPS mode since V_{th} is proportional to $1/d$, due to the increased surface anchoring effect. However, the decrease in transmittance is not equal to that of the IPS mode.

In order to find the origin of the decreased transmittance, it was necessary to investigate transmittance along the electrode position. Figure 6 shows the electrode position-dependent transmittance when the transmittance is maximum for three different cells. As clearly indicated by the arrows, the transmittance at the centre and edge of the electrode decreases with decreasing cell gap, which is the origin of the decreased transmittance for the cell with a 2 μm gap compared with the cell with a 4 μm gap. To understand the voltage-dependent transmittance along electrodes in more detail for cells with different cell gaps, we investigated the electrode-position dependent transmittance when applied voltages were, $V_{\text{op}}-0.5$ V (V_-), V_{op}, and $V_{\text{op}}+0.5$ V (V_+), as shown in figure 7. When the cell

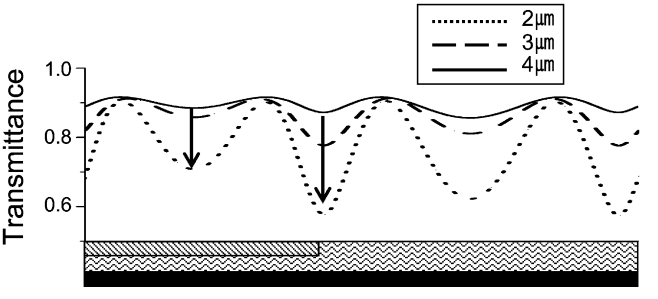

Figure 6. Comparison of the transmittance distribution of the white state along the electrode when the cell gap is 2, 3, and 4 μm.

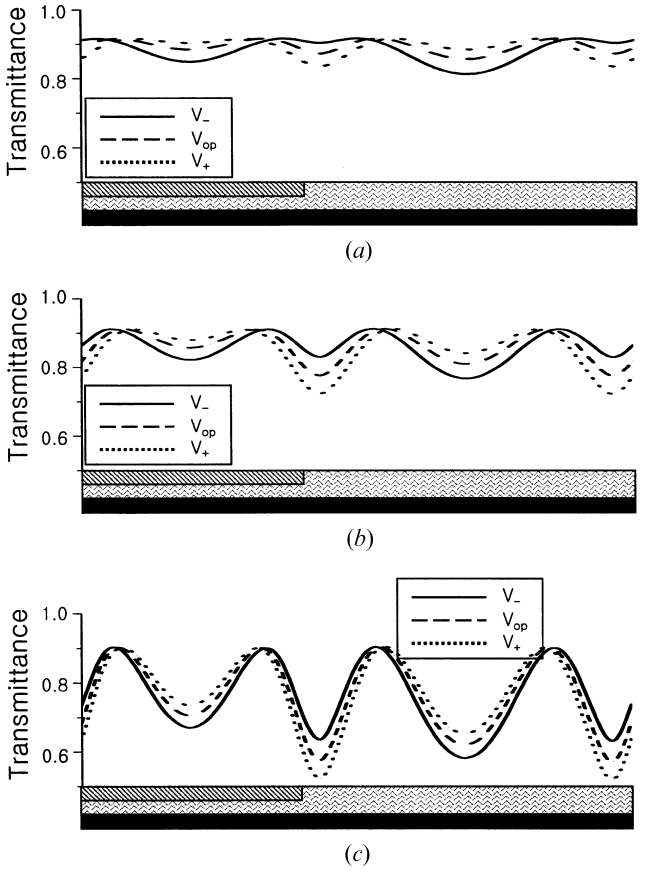

Figure 7. Transmittance distribution along electrodes at three different voltages when the cell gap is (*a*) 4 μm, (*b*) 3 μm, and (*c*) 2 μm.

gap is 4 μm, the transmittance at position *c* is higher than that at position *a* for an applied voltage of V_-. Further increasing the voltage to V_+, the transmittance at position *c* decreases, whereas it increases at position *a*, indicating that the LC at position *c* becomes overtwisted with increasing voltage but the LC at position *a* becomes properly twisted with increasing voltage. However, the transmittance difference between the two positions is not large. This also shows that the intensities of the dielectric and elastic torques is well balanced, giving rise to high transmittance at different positions. When the cell gap is 3 μm, a similar behaviour is seen, except that the transmittance difference between two positions at V_+ becomes large compared with the cell with a 4 μm cell gap. This indicates, that in order for the LC at position *a* to be properly twisted generating a maximum transmittance, the LC at the edge of the electrodes should be overtwisted.

When the cell gap is 2 μm, the transmittance at the centre and the edge of electrodes is much lower than for the cells having 3 or 4 μm cell gaps, at all three voltages. Further, even at V_-, the LC is overtwisted at the edge of the electrode, whereas it is undertwisted at position *a*, resulting in lower transmittance at the two positions than for the cells with 3 and 4 μm cell gaps. On increasing the voltage from V_- to V_+, the transmittance at position *c* decreases, while it continues to increase at position *a*. This indicates that the intensity of dielectric torque at position *c* and the elastic torque on the LC at position *a* do not match to generate maximum transmittance at the same time. In other words, at a voltage higher than V_+, the LC at position *a* can be twisted further, giving rise to increased transmittance; however the transmittance at position *c* is greatly decreased by overtwisting the LC, giving rise to a decreased average transmittance.

It can be understood that the low transmittance at position *a* is the result of competition between the elastic torque needed to twist the LC, and the elastic force needed to hold the LC in its initial state by surface anchoring. In other words, the LC at position *a* cannot be twisted easily due to the increased surface anchoring effect that occurs with a decreasing cell gap. Therefore, for the cell with a 2 μm gap, the field intensity needed to rotate the LC using dielectric torque, and the surface effect required to hold the LC in the initial state, is stronger than it is in the cell with a 4 μm gap. Thus the LC at position *a* cannot be twisted sufficiently, since the elastic torque cannot overcome the elastic force holding the LC in the initial state while the increased field intensity at position *c* overtwists the LC.

To understand the electrode position-dependent transmittance as a function of applied voltage and cell gap, in detail, we have calculated a director profile for the LC along the cell gap. Figure 8 shows the twist angle as a function of applied voltage for three different positions *a*, *b* and *c*, when the cell gap is 2 and 4 μm. At position *a*, the maximum twist angle occurs at z/d=0.5 and increases to 47° at 5.5 V (V_{op}) for the 2 μm cell, while it occurs at z/d=0.37 and increases to 60° at 4.5 V (V_{op}) for the 4 μm cell, indicating that the LC is twisted from its initial alignment by 35° for the 2 μm cell and 48° for the 4 μm cell. At position *c*, for the 2 μm cell, the maximum twist angle occurs around z/d=0.35 with values of 55° at 3 V and 79° at 5.5 V, indicating that the angle of twist from the applied voltage already reaches 45° at 3 V and exceeds 45° at greater voltages. Unlike in the 2 μm cell, in the 4 μm cell the maximum twist angle occurs at around z/d=0.2 with a value of 77° at 4.5 V. At position *b*, it occurs at z/d=0.5 with a value of 57° at 5.5 V for the 2 μm cell, and at z/d=0.35 with a value of 65° at 4.5 V for the 4 μm cell, indicating that the LCs are twisted by 45° and 53° from the initial alignment for the 2 μm and 4 μm cells, respectively.

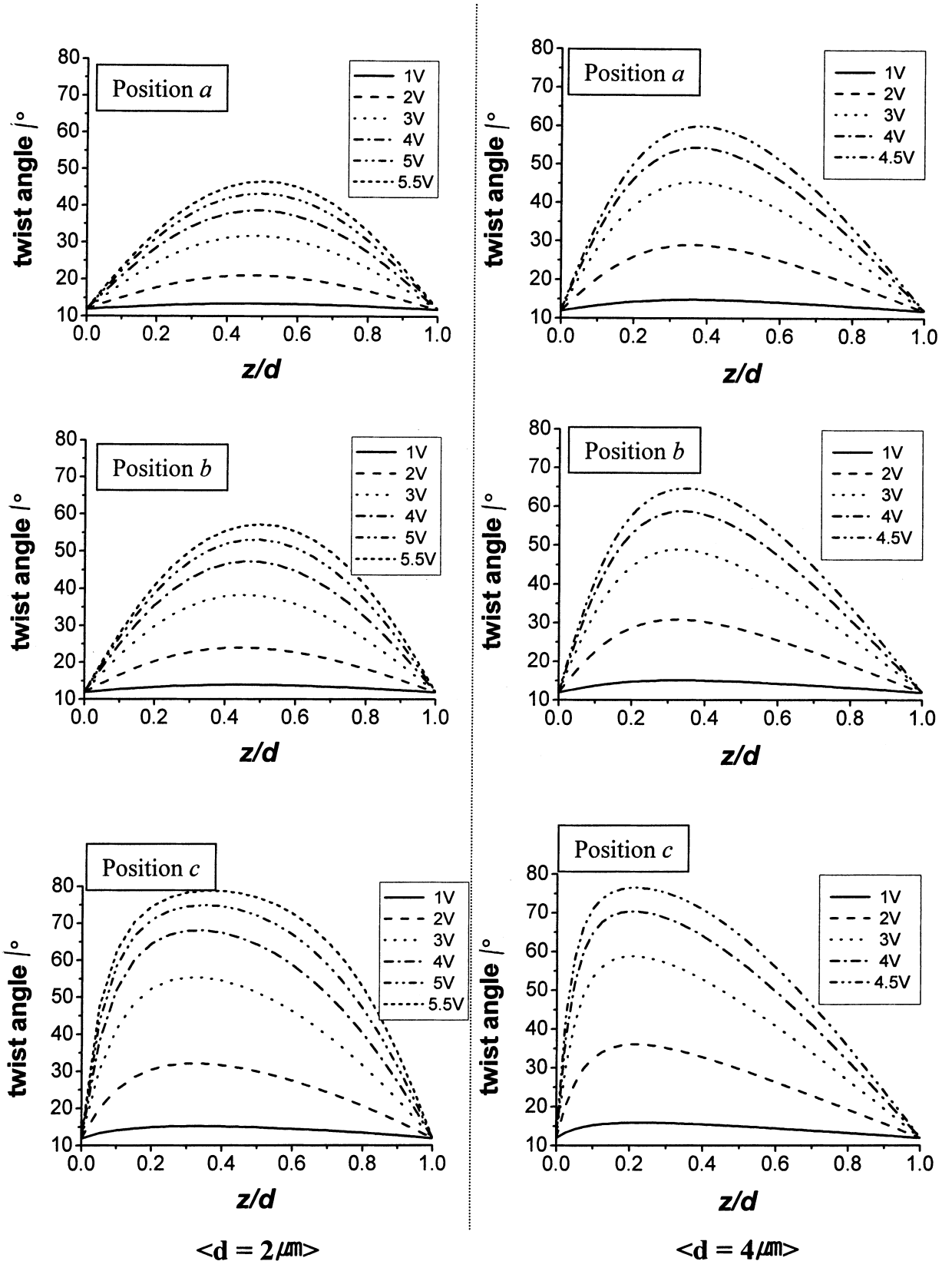

Figure 8. Distribution of the LC twist angle as a function of applied voltage at three different positions *a*, *b*, *c* when the cell gap is 2 and 4 μm.

The tilt angle, which is also an important factor affecting the cell retardation value and the electro-optic characteristics, is calculated for the same positions when V_{op} is applied, as shown in figure 9. For the cell with a 4 μm cell gap, the tilt angle at position *a* is very low since the vertical field intensity holds down the LC, whereas the LC at position *c* has a relatively high tilt angle of -14° near the bottom substrate, decreasing rapidly on moving away from the bottom substrate. The tilt angle of the mid-director is largest at position *b*, though its value is only about -2°. From this, one can understand that most of the LC tilt angles occur near the bottom substrates since the electrode exists only on the bottom substrates. When the cell gap decreases from 4 to 2 μm, the tilt angle along the vertical LC layer increases such that the tilt angle of the mid-director at positions *b* and *c* increases from -2° to -8°, and from -0° to -4°, respectively. Nevertheless, the degree of tilt is not so large that the transmittance is determined by the degree of the LC twist. Therefore, the explanations of the transmittance taking account only of twist angle are reasonable.

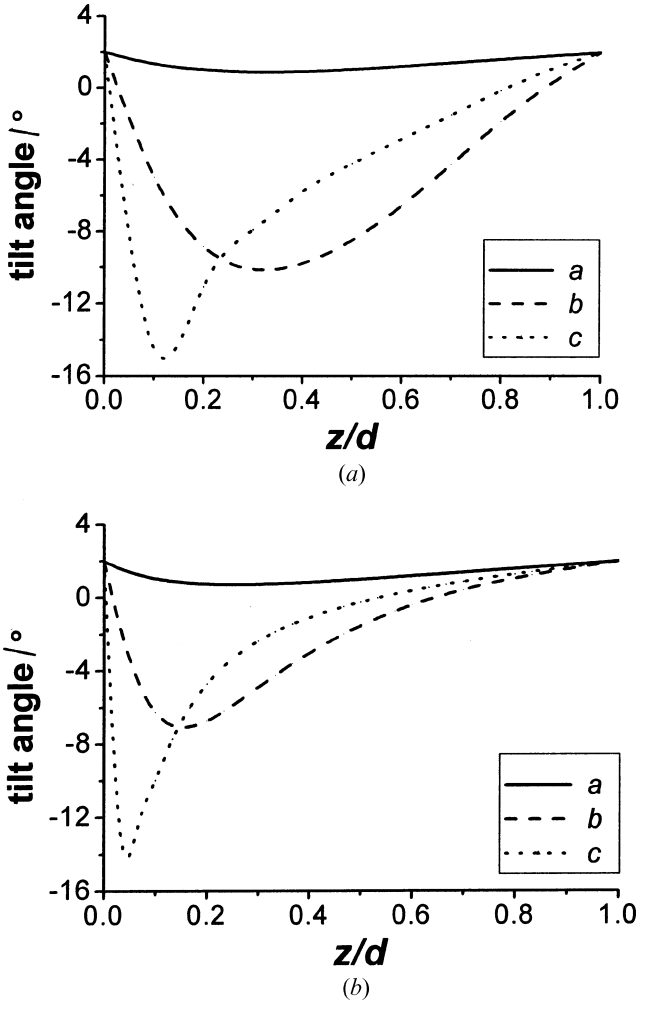

Figure 9. Distribution of the LC tilt angle at three different positions *a*, *b*, *c* when the cell gap is (*a*) 2 μm, and (*b*) 4 μm.

Now, from the local orientation of the LC twist angle, the transmittance at different electrode positions may be explained. From equation (1) one can clearly understand that the LC at position *a* is not twisted sufficiently to transmit light fully for a 2 μm cell whereas the LC at position *c* is overtwisted, resulting in low transmittance. However, the LC at electrode position *b*, is twisted sufficiently to generate maximum transmittance. Now, consider the transmittance of the cell with 4 μm cell gap; the LC is twisted enough to transmit light fully at electrode position *a*, and in addition, the transmittance is very high even at electrode position *c* although the twist angle is 65° at $z/d=0.2$, which is about the same value as in the cell with a 2 μm cell gap. According to equation (1), the transmittance at positions *a* and *c* should differ greatly since ψ has a large difference. However, the difference in transmittance is small because the LC profile at the edge of the electrode is like that of a low twisted nematic (TN) and therefore the transmittance follows the Gooch and Tarry TN behavior [11] instead of behaving as equation (1) predicts [14].

4. Experimental results and discussion

To confirm these calculated results, test cells were fabricated. The electrode width and the distance between electrodes are 3 and 5.5 μm, respectively. Two LC cells with cell gaps of 2.1 and 3.9 μm were also made. LC1 ($\Delta n=0.1547$ at $\lambda=589$ nm) and LC2 ($\Delta n=0.0785$ at $\lambda=589$ nm) were filled into the cells with 2.1 and 3.9 μm

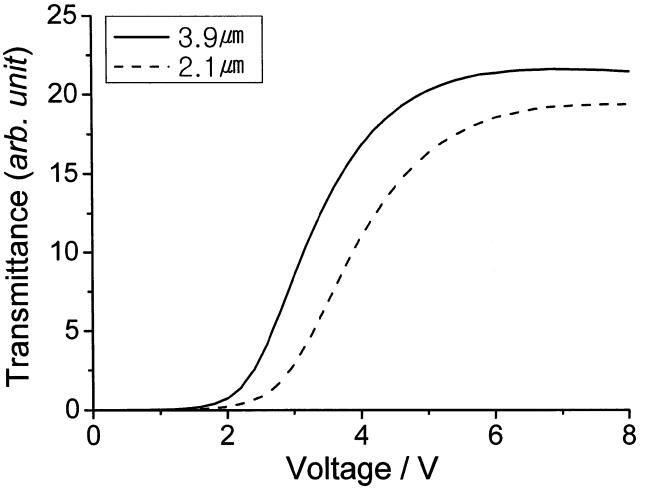

Figure 10. Measured voltage-dependent transmittance curves for cells with different cell gaps.

cell gap, respectively. As a result, the cell retardation values for the two cells were, respectively, 0.32 and 0.31 μm.

For the electro-optic measurements, a Halogen lamp was used as a light source and a square wave, 60 Hz voltage source from a function generator, was applied to the sample cell. Light passing through the cell was detected by a photomultiplier tube at room temperature.

Figure 10 shows voltage-dependent transmittance curves for the two different cells. As expected, the V_{th} and V_{op} are higher for the 2.1 μm cell than for the 3.9 μm cell; also the 2.1 μm cell shows a slightly lower transmittance than the 3.9 μm cell, although the first has a slightly higher cell retardation value than the latter, which agrees with calculated results. To understand how the LC director reacts to an applied voltage along the electrode, the voltage-dependent LC texture was observed using polarizing optical microscopy. Here, the light source intensity was adjusted to show contrast along the electrodes. Figure 11 shows photomicrographs of the cell, together with the calculated transmittance profile.

For the 2.1 μm cell, the mid-grey transmittance is highest (about 0.8) for position *c*, low (about 0.38) for position *a* and lowest (about 0.2) for position *d* of the calculated results, which agree with the experimental results. Increasing the voltage to white-state, the transmittance at position *c* decreases to about 0.6 while the transmittance at positions *a* and *d* increases to about 0.7 and 0.46, respectively, for the calculated results. Again, the observed results agree with calculated

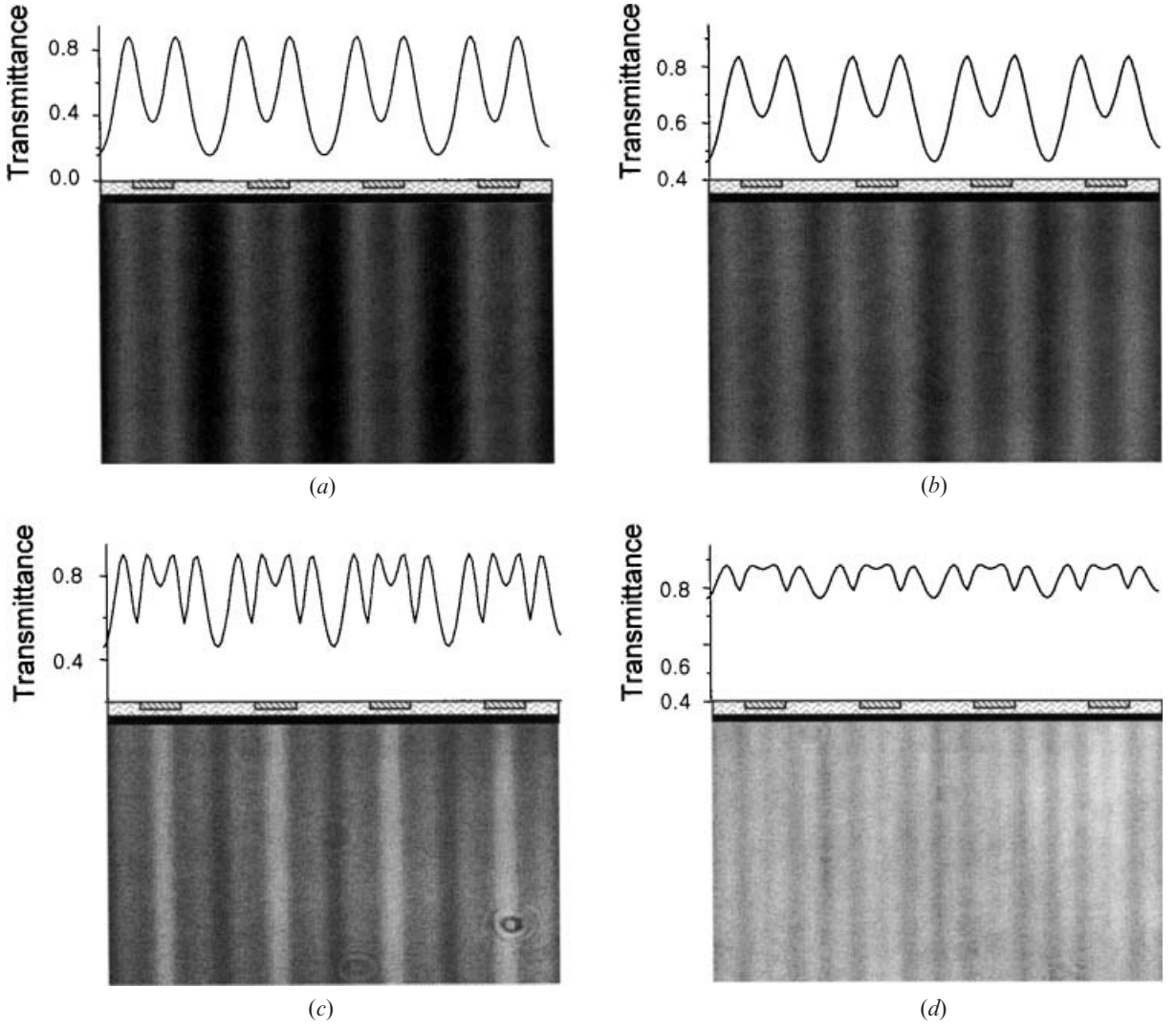

Figure 11. Photomicrograph of the FFS cells showing how the intensity of transmittance changes along the electrodes at mid-grey with cell gaps of (*a*) 2.1 μm and (*b*) 3.9 μm; and at white state with cell gaps of (*c*) 2.1 μm and (*d*) 3.9 μm. The calculated results of transmittance along electrodes above the textures show good agreement.

results. The reason for the lower transmittance at position *d* compared with that at position *a*, is that the electrode width of an opened common electrode is wider than that of the pixel electrode. In other words, with greater electrode width, the equipotential surface increases, resulting in less electric torque on the LC at position *d*.

For the 3.9 μm cell, transmittance at mid-grey is highest for position *c* and lowest for position *d*. In addition, the transmittance at position *a* is higher than that at position *d*. However, at white-state, the transmittance at position *c* and *d* is slightly lower than at position *a*, but the transmittance for all positions remains high, over 0.8, unlike the cell with the lower cell gap.

From these observations, the results can be summarized: first, the experimental results show clearly that the total transmittance of the FFS cell with a large cell gap is higher than that with a small cell gap. Secondly, the reason for the lower transmittance at position *d* compared with position *a* for both cells, is that the LCs are not fully twisted due to weak elastic torque on the LCs at position *d*. Because of the wider electrode dimensions, the lower elastic torque acts on the LCs due to the increased equipotential surface. Further, for the cell with the smaller cell gap, the elastic torque is negatively affected by the increased surface anchoring effect. Thirdly, the dielectric and elastic torque are not balanced for the cell with a small cell gap, resulting in low transmittance.

5. Conclusion

Voltage-dependent transmittance and LC deformation, as a function of cell gap, have been studied for the FFS mode when an LC with negative dielectric anisotropy is used. In the FFS mode, when cell gap decreases from 4 to 2 μm, the transmittance of the 2 μm cell becomes strongly dependent on the electrode position, resulting in a lower transmittance compared with the 4 μm cell. The transmittance at the centre of pixel and common electrode is particularly low due to the increased surface anchoring effect holding the LC in the initial state. Unlike conventional LC cells such as IPS and TN devices, the two torques, dielectric and elastic, cause the homogeneously aligned LCs to twist sequentially. Therefore, when the cell gap becomes very small, competition between the elastic torque to twist the LC and elastic force to hold the LC at its initial state occurs. Consequently, the LCs at the centre of the pixel and common electrodes, in which no horizontal field exists, are not twisted sufficiently, resulting in low transmittance. This result is very important when designing an FFS mode with high light efficiency.

Acknowledgements

This work was performed by the Advanced Backbone IT development project supported by the Ministry of Information & Communication in the Republic of Korea.

References

[1] B. Kiefer, B. Weber, F. Windsceid, G. Baur. In *Proceeding of the 12th International Display Research Conference* (Society for Information Display and the Institute of Television Engineers of Japan, Hiroshima), 547 (1992).
[2] M. Oh-e, K. Kondo. *Appl. Phys. Lett.*, **67**, 3895 (1995).
[3] K. Kondo, S. Matsuyama, N. Konishi, H. Kawakami. In *Digest of Technical Papers of 1998 Society for Information Display International Symposium*, Anaheim, 389 (1998).
[4] H.Y. Kim, I.S. Song, S.H. Lee. *Trans. EEM*, **4**, 24 (2003).
[5] S.H. Lee, S.L. Lee, H.Y. Kim. In *Proceeding of the 18th International Display Research Conference* (Society for Information Display and the Institute of Television Engineers of Japan, Hiroshima), 371 (1998).
[6] S.H. Lee, S.L. Lee, H.Y. Kim. *Appl. Phys. Lett.*, **73**, 2881 (1998).
[7] S.H. Hong, I.C. Park, H.Y. Kim, S.H. Lee. *Jpn. J. appl. Phys.*, **39**, L527 (2000).
[8] S.H. Lee, S.M. Lee, H.Y. Kim, J.M. Kim, S.H. Hong, Y.H. Jeong, C.H. Park, Y.J. Choi, J.Y. Lee, J.W. Koh, H.S. Park. In *Digest of Technical Papers of 2001 Society for Information Display International Symposium*, San Jose, 484 (2001).
[9] H.Y. Kim, S.H. Nam, S.H. Lee. *Jpn. J. appl. Phys.*, **42**, 2752 (2003).
[10] J.-D. Noh, H.Y. Kim, J.M. Kim, J.W. Koh, J.Y. Lee, H.S. Park, S.H. Lee. In *Digest of Technical Papers of 2002 Society for Information Display International Symposium*, Boston, 224 (2002).
[11] C. Gooch, H.A. Tarry. *J. Phys. D*, **8**, 1575 (1975).
[12] S.H. Lee, S.L. Lee, H.Y. Kim, T.Y. Eom. *J. Kor. phys. Soc.*, **35**, S1111 (1999).
[13] A. Lien. *Appl. Phys. Lett.*, **57**, 2767 (1990).
[14] S.H. Jung, H.Y. Kim, J.H. Kim, S.-H. Nam, S.H. Lee. *Jpn. J. appl. Phys.*, **43**, 1028 (2004).